








In the format provided by the authors and unedited.








GABA and glutamate neurons in the VTA regulate sleep and wakefulness

Xiao Yu ^{1,8}, Wen Li^{2,8}, Ying Ma ¹, Kyoko Tossell¹, Julia J. Harris^{1,3}, Edward C. Harding ¹,
Wei Ba¹, Giulia Miracca¹, Dan Wang², Long Li², Juan Guo², Ming Chen⁴, Yuqi Li¹, Raquel Yustos¹,
Alexei L. Vyssotski⁵, Denis Burdakov ³, Qianzi Yang², Hailong Dong ^{2*}, Nicholas P. Franks ^{1,6,7*} and
William Wisden ^{1,6,7*}

¹Department of Life Sciences, Imperial College London, London, UK. ²Department of Anesthesiology & Perioperative Medicine, Xijing Hospital, Xi'an, Shanxi, China. ³The Francis Crick Institute, London, UK. ⁴Human Institute, ShanghaiTech University, Shanghai, China. ⁵Institute of Neuroinformatics, University of Zürich/ETH Zürich, Zürich, Switzerland. ⁶Centre for Neurotechnology, Imperial College London, London, UK. ⁷UK Dementia Research Institute, Imperial College London, London, UK. ⁸These authors contributed equally: Xiao Yu, Wen Li. *e-mail: hldong6@hotmail.com; n.franks@imperial.ac.uk; w.wisden@imperial.ac.uk

In the format provided by the authors and unedited.

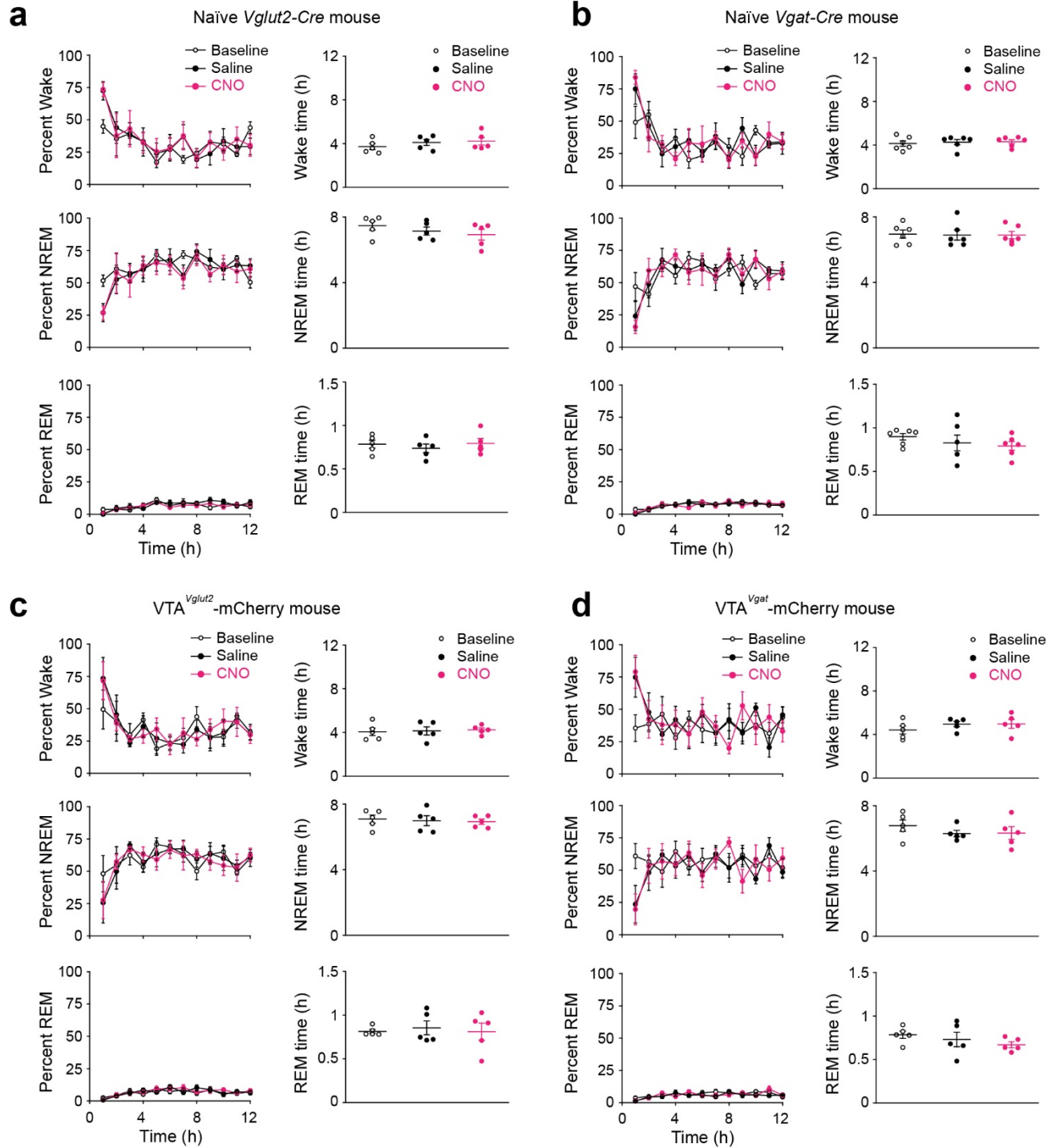
GABA and glutamate neurons in the VTA regulate sleep and wakefulness

Xiao Yu ^{1,8}, Wen Li^{2,8}, Ying Ma ¹, Kyoko Tossell¹, Julia J. Harris^{1,3}, Edward C. Harding ¹,
Wei Ba¹, Giulia Miracca¹, Dan Wang², Long Li², Juan Guo², Ming Chen⁴, Yuqi Li¹, Raquel Yustos¹,
Alexei L. Vyssotski⁵, Denis Burdakov ³, Qianzi Yang², Hailong Dong ^{2*}, Nicholas P. Franks ^{1,6,7*} and
William Wisden ^{1,6,7*}

¹Department of Life Sciences, Imperial College London, London, UK. ²Department of Anesthesiology & Perioperative Medicine, Xijing Hospital, Xi'an, Shanxi, China. ³The Francis Crick Institute, London, UK. ⁴Human Institute, ShanghaiTech University, Shanghai, China. ⁵Institute of Neuroinformatics, University of Zürich/ETH Zürich, Zürich, Switzerland. ⁶Centre for Neurotechnology, Imperial College London, London, UK. ⁷UK Dementia Research Institute, Imperial College London, London, UK. ⁸These authors contributed equally: Xiao Yu, Wen Li. *e-mail: hldong6@hotmail.com; n.franks@imperial.ac.uk; w.wisden@imperial.ac.uk

Supplementary Information

CNO control

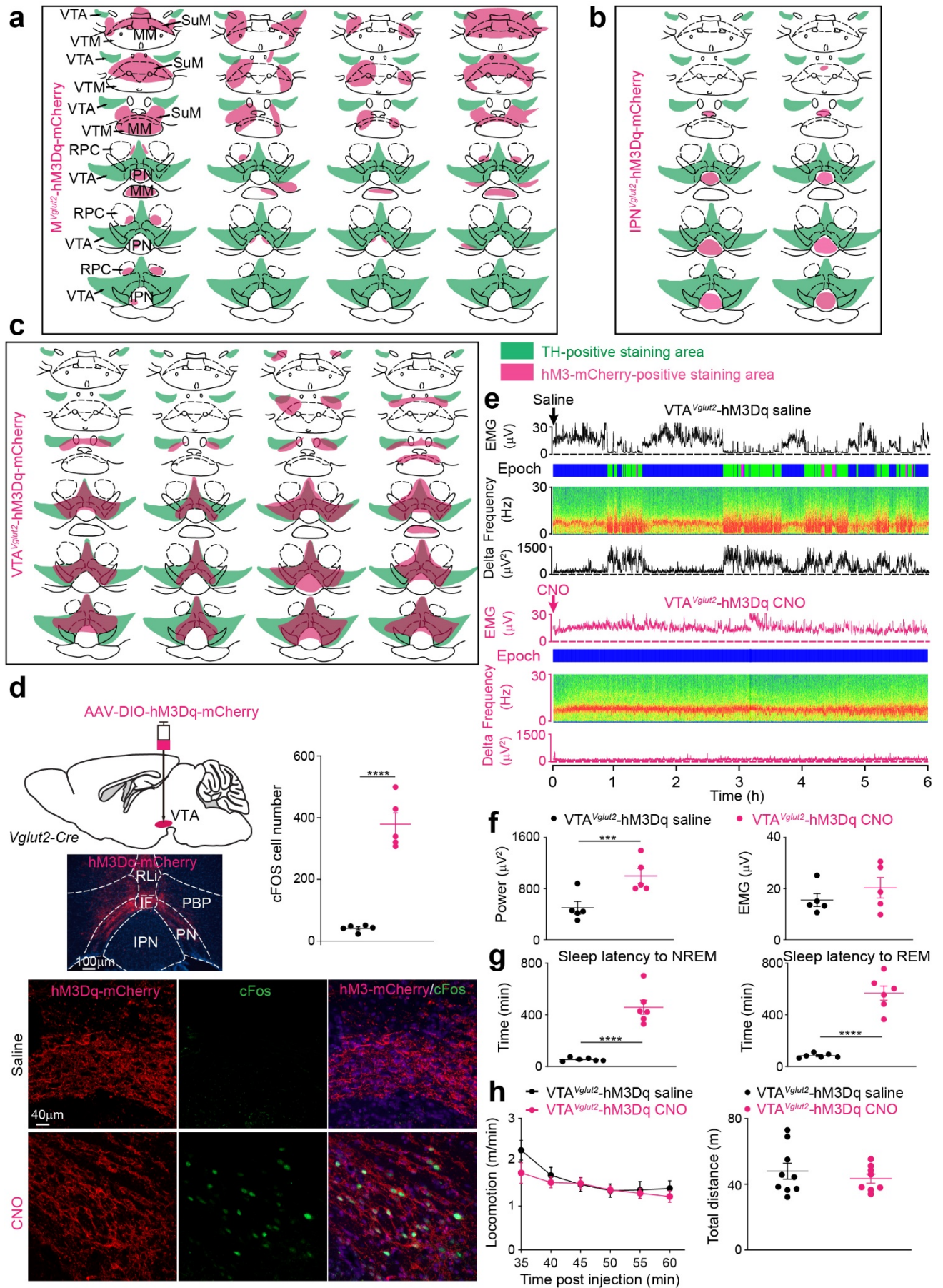


Supplementary Fig. 1 (Associated with Fig. 1, 3, 5, 7) CNO (1 mg/kg) controls for *Vglut2-ires-Cre* and *Vgat-ires-Cre* mice. CNO does not alter the amount of sleep or wake in the background strains of mice used in the study.

(a, b) Saline or CNO (1 mg/kg) was injected *i.p.* into *Vglut2-ires-Cre* mice (n=5 mice) (a) or *Vgat-ires-Cre* mice (n=6 mice) (b) which had not received any AAV injections. Percentage and time of wake, NREM and REM sleep were scored during the baseline sleep-wake cycle or after saline or CNO injection.

(c, d) AAV-DIO-mCherry was injected into the VTA of *Vglut2-ires-Cre* mice (n=5 mice) (c) or *Vgat-ires-Cre* mice (n=5 mice) (d). Percentage and time of wake, NREM and REM sleep were scored during the baseline sleep-wake cycle or after saline or CNO *i.p.* injection.

p>0.05, repeated measures one-way ANOVA and Bonferroni-Holm *post hoc* test. All error bars represent the SEM. For detailed statistics information, see Supplementary Table1.



Supplementary Fig. 2 (Associated with Fig. 1)

Examples of expression of hM3Dq-mCherry expression in individual *Vglut2-Cre* mice

(a, b, c) hM3Dq-mCherry expression in individual *Vglut2-Cre* mice. Coronal brain sections shown as line diagrams from individual mice, from anterior to posterior, with areas of hM3Dq-mCherry receptor expression, shown schematically in magenta, in M^{Vglut2} -hM3Dq, IPN^{Vglut2} -hM3Dq and VTA^{Vglut2} -hM3Dq mice. Green indicates tyrosine hydroxylase (TH) staining. IPN, interpeduncular nucleus; MM, medial mammillary area; RPC, red nucleus, parvocellular part. SuM, supramammillary area. VTM, ventral tuberomammillary nucleus.

Chemogenetic activation of VTA^{Vglut2} neurons in VTA^{Vglut2} -hM3Dq mice promotes wakefulness but without hyperlocomotion

(d) One hour after CNO *i.p.* injection into VTA^{Vglut2} -hM3Dq mice, cFOS protein was elevated in hM3Dq-expressing VTA^{Vglut2} neurons (saline, n=5 mice; CNO, n=5 mice). Immunohistochemistry for hM3Dq-mCherry expression and cFOS in VTA^{Vglut2} neurons of VTA^{Vglut2} -hM3Dq mice 1 hour after CNO or saline *i.p.* injections. IF, interfascicular nucleus; RLi, rostral linear nucleus; PBP, parabrachial pigmented nucleus; PN, paranigral nucleus; IPN, interpeduncular nucleus.

(e) Example of EMG, EEG and δ power spectra of VTA^{Vglut2} -hM3Dq mice that had received saline or CNO *i.p.* injection. "Epoch" indicates the vigilance state: blue, wake; green, NREM sleep; magenta, REM sleep.

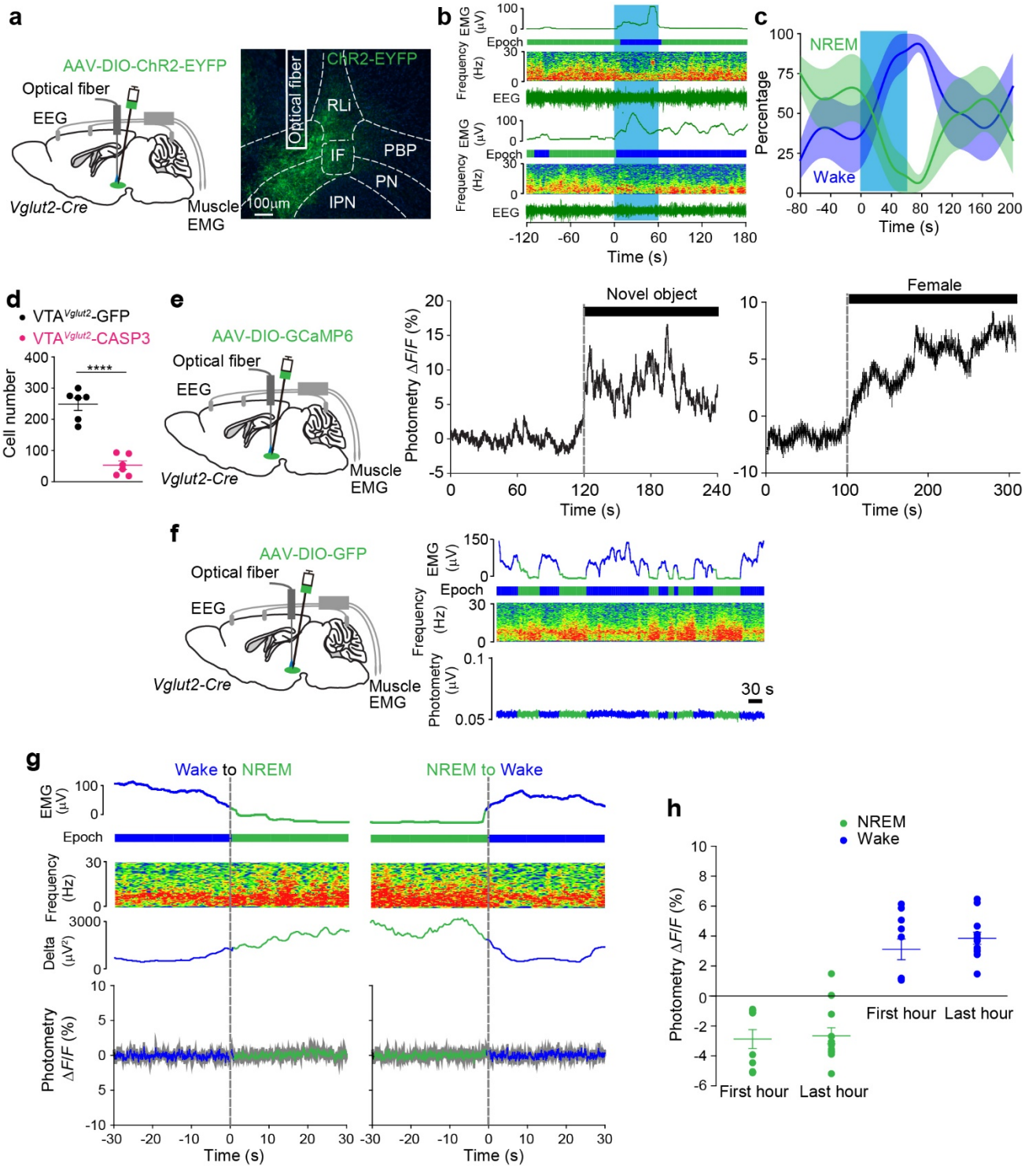
(f) Theta power and EMG amplitude of VTA^{Vglut2} -hM3Dq mice that had received saline (n=5 mice) or CNO (n=5 mice) *i.p.* injections.

(g) Latency to NREM and REM sleep for VTA^{Vglut2} -hM3Dq mice that had received saline (n=6 mice) or CNO (n=6 mice) *i.p.* injections.

(h) Locomotor speed and distance travelled of VTA^{Vglut2}-hM3Dq mice that had received saline (n=9 mice) or CNO (n=8 mice) *i.p.* injections.

p<0.001, *p<0.0001; two-sided unpaired t-test. Error bars represent the SEM.

For detailed statistics information, see Supplementary Table1.



Supplementary Fig. 3 (Associated with Fig 1, 2, 3)

Optogenetic activation of VTA^{Vglut2} neurons promotes wakefulness

(a) Immunohistochemistry for ChR2-EYFP expression in VTA^{Vglut2} neurons of VTA^{Vglut2}-ChR2-EYFP mice and the track of optical fiber placement. The experiment was repeated independently 3 times. IF, interfascicular nucleus; RLi, rostral linear nucleus; PBP, parabrachial pigmented nucleus; PN, paranigral nucleus; IPN, interpeduncular nucleus.

(b) Example of EMG, EEG, epoch and EEG spectra of two VTA^{Vglut2}-ChR2-EYFP mice that had opto-activation. “Epoch” indicates the vigilance state: blue, wake; green, NREM sleep; magenta, REM sleep.

(c) Percentage of wake and NREM sleep of VTA^{Vglut2}-ChR2-EYFP mice (n=6 mice) that had opto-activation. The envelopes indicate the sem.

(d) Quantitative assessment of VTA^{Vglut2} lesioning. GFP-positive cell numbers of VTA^{Vglut2}-GFP mice (n=6 mice) and VTA^{Vglut2}-CASP3 mice (n=6 mice).

Additional photometry data for VTA^{Vglut2}-GCaMP6 mice and control photometry data (VTA^{Vglut2}-GFP mice)

(e) Ca²⁺ photometry signal of VTA^{Vglut2} neurons in VTA^{Vglut2}-GCaMP6 mice in the presence of novel objects and female mice.

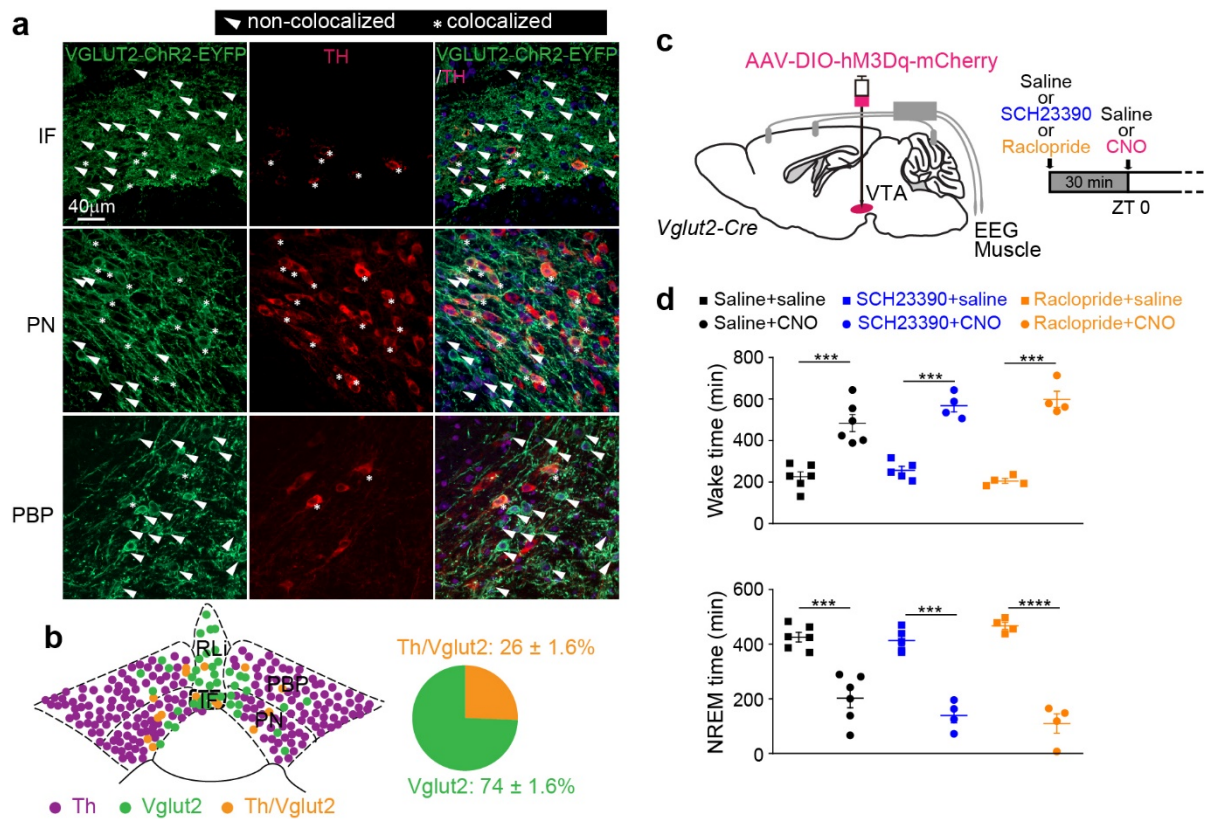
(f) Photometry control. Injection of AAV-DIO-GFP into the VTA of the *Vglut2-ires-Cre* mice. Ca²⁺ photometry spectra (bottom trace) recorded in the VTA of VTA^{Vglut2}-GFP mice aligned with the EEG (middle trace) and EMG (top trace) during wakefulness and NREM sleep. “Epoch” indicates the vigilance state: blue, wake; green, NREM sleep; magenta, REM sleep.

(g) Photometry control. Ca²⁺ signal in *Vglut2* neurons of VTA^{Vglut2}-GFP mice at the boundaries of the vigilance states. Ca²⁺ photometry $\Delta F/F$ ratio (bottom trace) in the VTA^{Vglut2}-GFP mice aligned with the extracted δ power in the EEG, the EEG spectra

and EMG during wakefulness and NREM sleep. “Epoch” indicates the vigilance state: blue, wake; green, NREM sleep; magenta, REM sleep.

(h) Photometry signal of VTA^{Vglut2} neurons in VTA^{Vglut2}-GCaMP6 mice during the first hour (1 hr) (n=4 mice; 10 sessions) and last hour (6 hr) (n= 4 mice; 12 sessions) of recording.

****p<0.0001; for d, two-sided unpaired t-test; for h, repeated measures two-way ANOVA and Bonferroni-Holm *post hoc* test. All error bars represent the SEM. For detailed statistics information, see Supplementary Table1.



Supplementary Fig. 4 (Associated with Fig 1, 2, 3)

***Vglut2* and *Th* neurons in the VTA are mostly distinct**

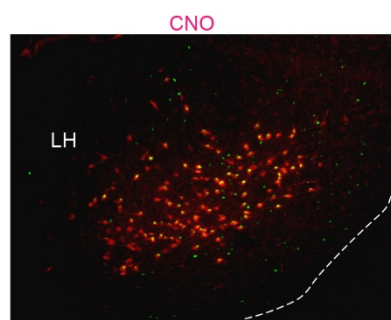
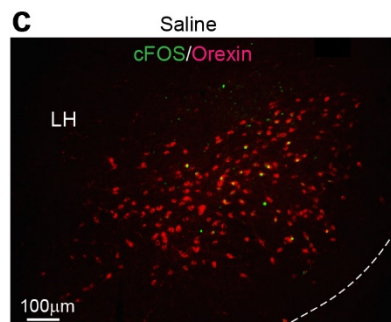
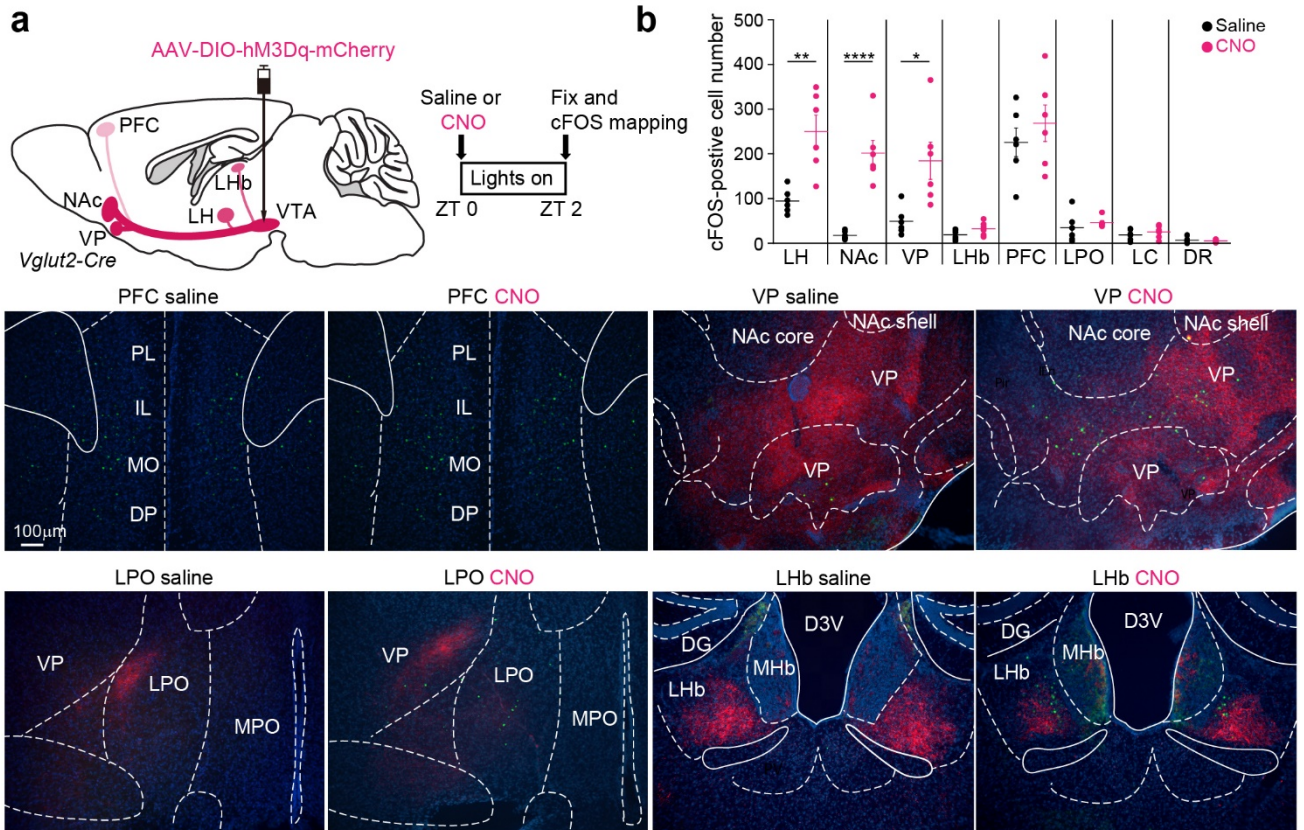
(a) Expression of ChR2-EYFP in tyrosine hydroxylase (TH)-positive neurons in the VTA of VTA^{Vglut2}-ChR2-EYFP mice. **The** experiment was repeated independently 4 times. IF, interfascicular nucleus; PN, paranigral nucleus; PBP, parabrachial pigment nucleus.

(b) Schematic of distribution of TH and *Vglut2* neurons and any colocalization in the VTA area (n=4 mice). RLi, rostral linear nucleus; PBP, parabrachial pigmented nucleus; PN, paranigral nucleus; IPN, interpeduncular nucleus. Data for pie chart represent as mean ± SEM.

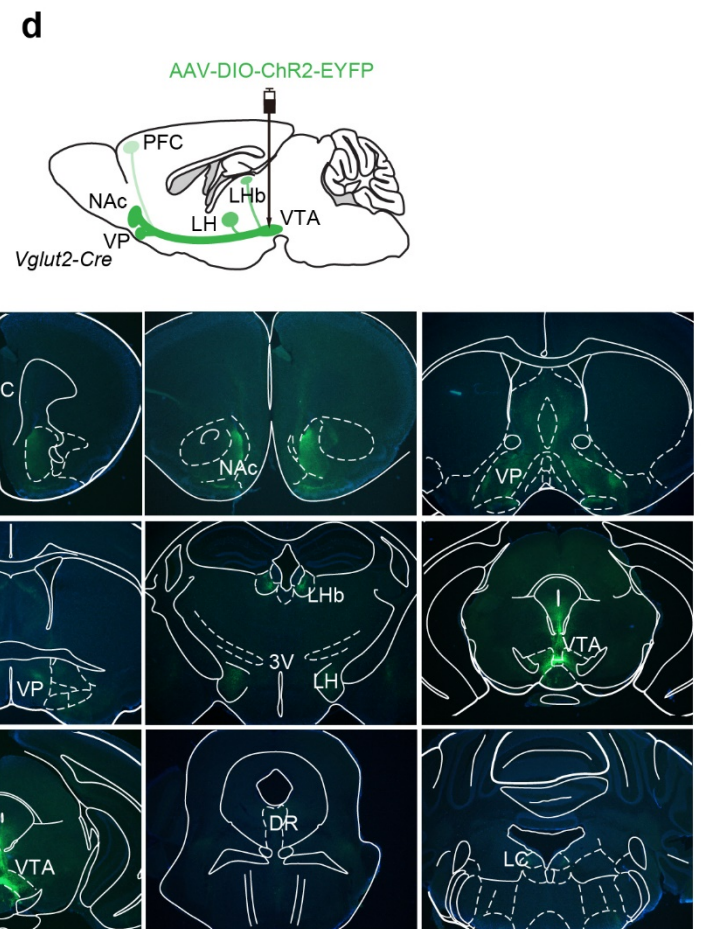
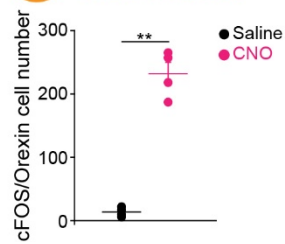
VTA^{Vglut2} neuron-induced wakefulness does not depend on dopamine receptor activation

(c) Dopamine receptor D1 and D2/3 receptor antagonists (SCH23390 and raclopride respectively) were injected *i.p.* into VTA^{Vglut2}-hM3Dq mice 30 min before CNO injection, which took place at ZT0, the start of the “lights on” period.

(d) Wake and NREM time scored for 12 hours after saline or CNO injection into VTA^{Vglut2}-hM3Dq mice in the presence of dopamine receptor antagonists or control saline. *** $p < 0.001$, **** $p < 0.0001$, repeated measures two-way ANOVA and Bonferroni-Holm *post hoc* test. All error bars represent the SEM. For detailed statistics information, see Supplementary Table1.



cFOS 40%
cFOS/Orexin 60%



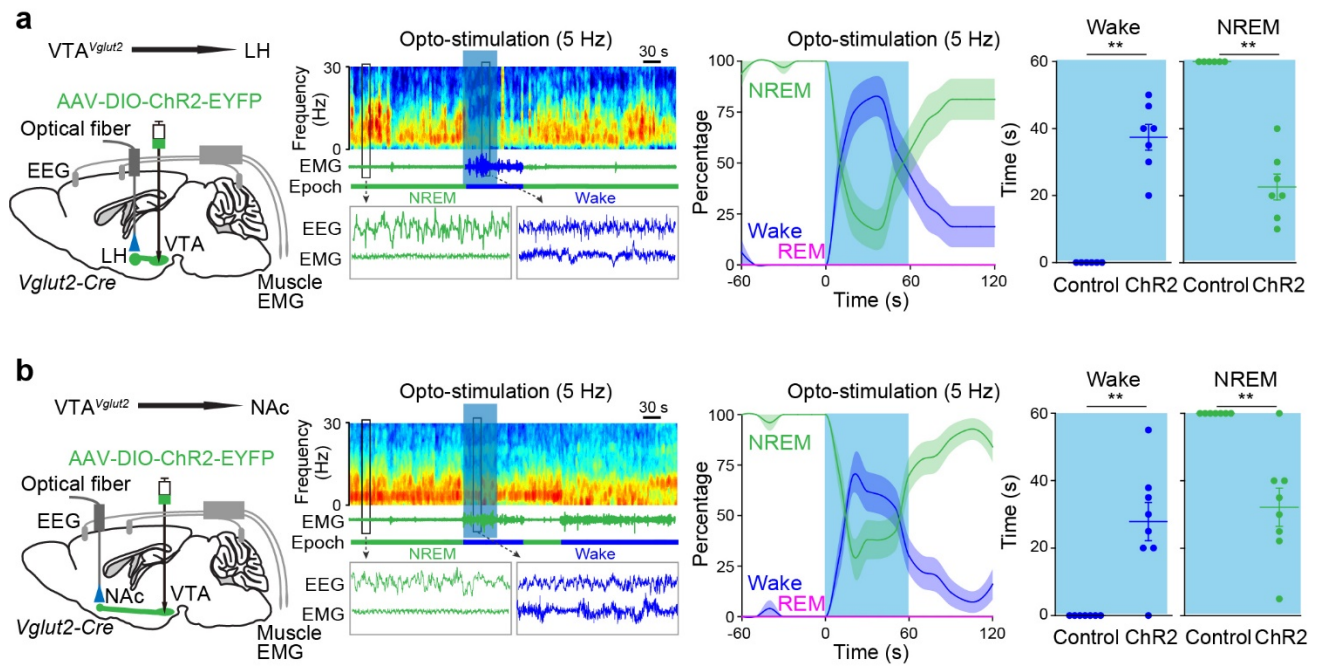
Supplementary Fig. 5 (Associated with Fig. 3) Chemogenetic and optogenetic circuit mapping of VTA^{Vglut2} neurons

(a, b) Chemogenetic mapping with cFOS expression following activation of VTA^{Vglut2} neurons. The number of cFOS neurons identified immunohistochemically (green dots) were counted (see graph in B) throughout the brain two hours after CNO (n=6 mice) or saline (n=6 mice) *i.p.* injection at ZT0 (start of “lights on”) in VTA^{Vglut2}-hM3Dq mice. The magenta staining is the primary fluorescence of VTA^{Vglut2} axons containing hM3Dq-mCherry protein.

(c) Double-labelling and quantification of cFOS and orexin expression by immunocytochemistry in the LH area of VTA^{Vglut2}-hM3Dq mice 2 hours after saline (n = 4 mice) or CNO *i.p.* injection (n = 4 mice).

(d) Circuit mapping for VTA^{Vglut2}-ChR2-EYFP mice in whole brain. PFC, prefrontal cortex. PL, prelimbic cortex; IL, infralimbic cortex; MO, medial orbitocortex; DP, dorsal peduncular cortex; VP, ventral pallidum; NAc, nucleus accumbens; LPO, lateral preoptic area; MPO, medial preoptic area; LH, lateral hypothalamus; DM, dorsomedial hypothalamus; PeF, perifornical region; MCLH, magnocellular nucleus, lateral hypothalamus; MTu, medial tuberomammillary nucleus; LHb, lateral habenula; MHb, medial habenula; DG, dentate granule cells; D3V, dorsal third ventricle; LC, locus ceruleus, LDT, lateral dorsal tegmental area; VTA ventral tegmental area; DR, dorsal raphe.

*p<0.05, **p<0.01, ****p<0.0001; two-sided unpaired t-test. Error bars represent the SEM. For detailed statistics information, see Supplementary Table1.

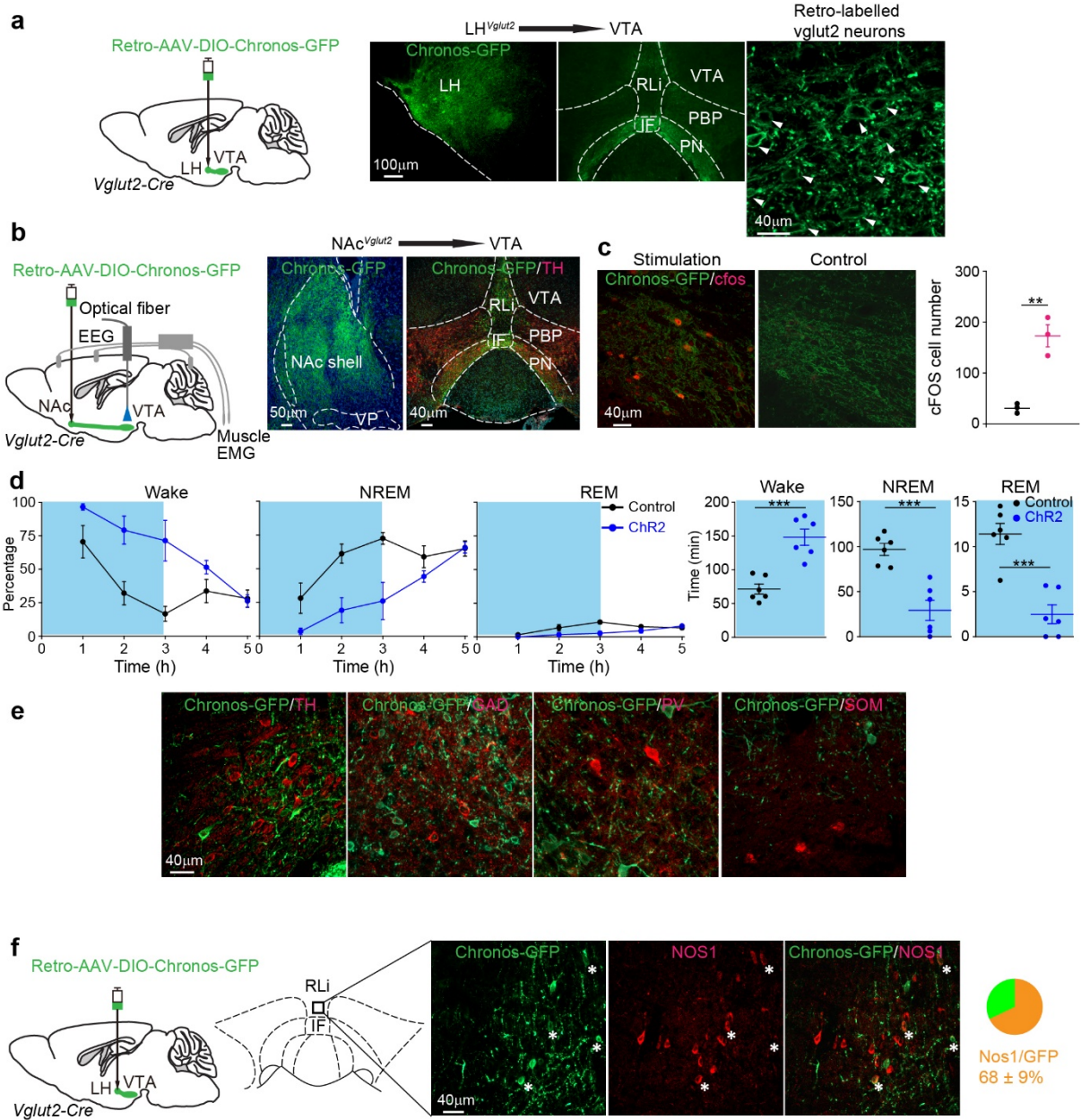


Supplementary Fig. 6 (Associated with Fig. 3) Optogenetic activation of VTA^{Vglut2}→LH or VTA^{Vglut2}→NAc projections

(a) For stimulating the VTA^{Vglut2}→LH projections, mice were given 60 s of opto-stimulation (5 Hz) during NREM sleep (“lights on” period) and the percentage and time of wake and NREM sleep were scored (control: n=6 mice; 13 trials; ChR2: n=7 mice; 30 trials).

(b) For stimulating the VTA^{Vglut2}→NAc projections, mice were given 60 s of opto-stimulation (5 Hz) during NREM sleep (“lights on” period) and the percentage and time of wake and NREM sleep were scored (control: n=7 mice; 18 trials; ChR2: n=8 mice; 25 trials).

**p<0.01, two-sided mann-whitney u test. All error bars represent the SEM. Shaded regions represent SEM. For detailed statistics information, see Supplementary Table1.



Supplementary Fig. 7 (Associated with Fig. 3)

Retro-labeling of VTA^{Vglut2}→LH and VTA^{Vglut2}→NAc projections

(a) Retro-AAV-DIO-Chronos-GFP was injected into the LH area of *Vglut2-ires-Cre* mice. Images show GFP staining in the LH and VTA areas. White arrows indicate retro-labeled soma in the VTA. The experiment was repeated independently 3 times.

(b) Retro-AAV-DIO-Chronos-GFP was injected into the NAc area of *Vglut2-ires-Cre* mice. Images show GFP staining in the NAc and VTA areas. The experiment was repeated independently 3 times.

Opto-activation of retro-labeled VTA^{Vglut2} neurons

(c) Chronos-GFP and cFOS expression in Chronos (n=3 mice) or control mice (n=3 mice) after 2 hours of opto-stimulation (20 Hz for 2 seconds with 58 seconds interval).

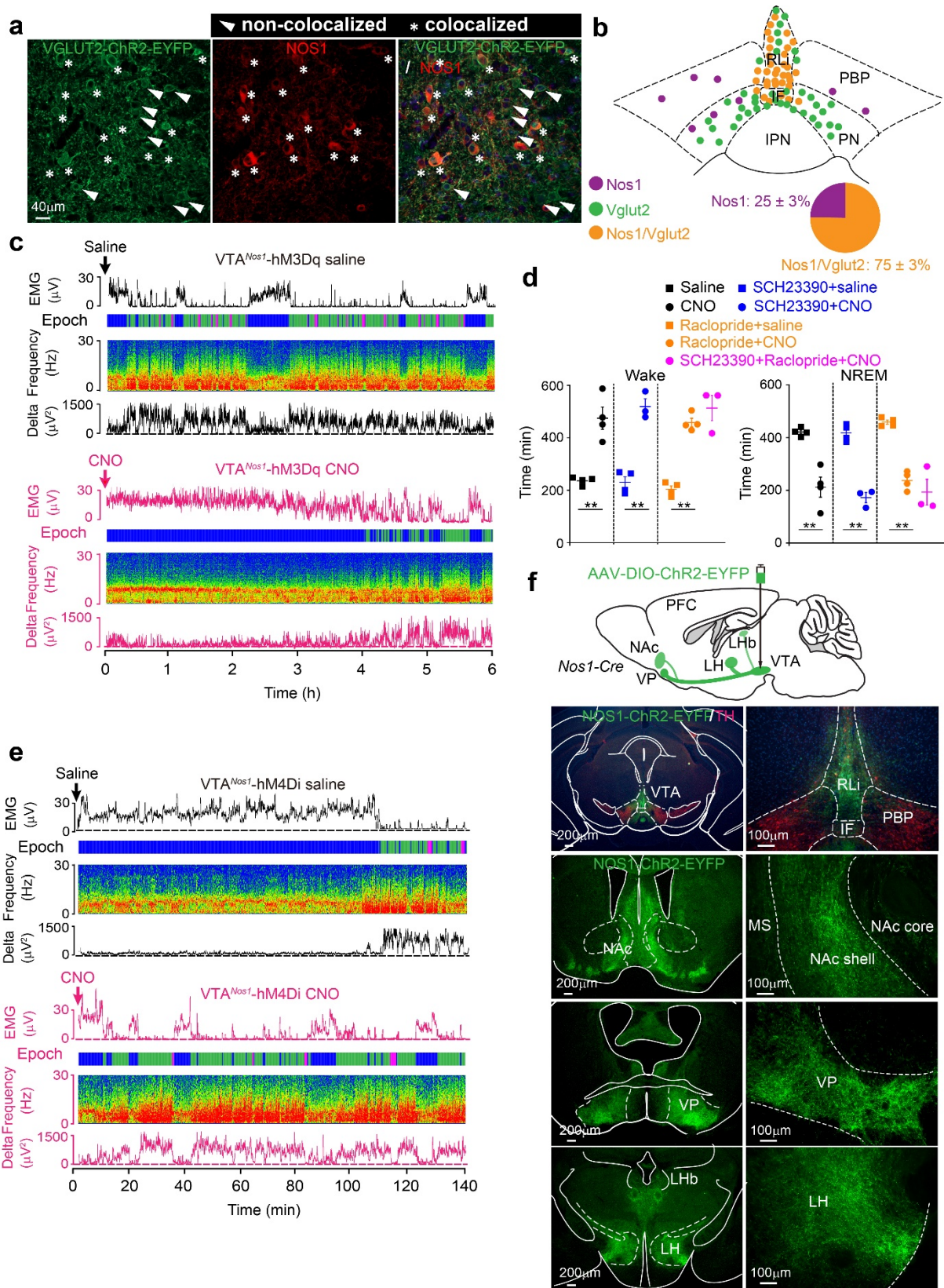
(d) An optical fiber was placed into the VTA area of Retro NAc^{Vglut2}-Chronos-GFP mice (n=6 mice) or control mice (n=6 mice), and mice were given 3 hours of opto-stimulation (20 Hz for 2 seconds with 58 seconds interval) and the percentage and time of wake, NREM and REM sleep were scored.

Identification of neuronal makers of retro-labeled VTA^{Vglut2} neurons

(e) Double labeling of retro-labeled VTA^{Vglut2} neurons with TH, GAD, PV or SOM. The experiment was repeated independently 3 times.

(f) Retro-AAV-DIO-Chronos-GFP was injected into the LH area of *Vglut2-ires-Cre* mice. Chronos-GFP expression was detected in cells of the VTA, and Chronos-GFP retro-labeled VTA midline soma (from LH injection) were doubled labelled with NOS1 (n= 4 mice). Data for pie chart represent as mean ± SEM.

p<0.01, *p<0.001; two-sided unpaired t-test. Error bars represent the SEM. For detailed statistics information, see Supplementary Table1.



Supplementary Fig. 8 (Associated with Fig. 3)

The majority of midline VTA^{Vglut2} neurons express NOS1

(a, b) Immunohistochemistry staining of midline VTA neurons in VTA^{Vglut2}-ChR2-EYFP mice with GFP and NOS1 (n = 3 mice). Data for pie chart represent mean ± SEM. The majority of *Nos1/Vglut2* neurons are in the midline VTA area (see schematic). IF, interfascicular nucleus; RLi, rostral linear nucleus; PBP, parabrachial pigmented nucleus; PN, paranigral nucleus; IPN, interpeduncular nucleus.

VTA^{Nos1} induced wakefulness is independent of dopamine activation

(c) Examples of EEG, EMG and delta power spectra from CNO or saline-injected VTA^{Nos1}-hM3Dq mice. “Epoch” indicates the vigilance state: blue, wake; green, NREM sleep; magenta, REM sleep.

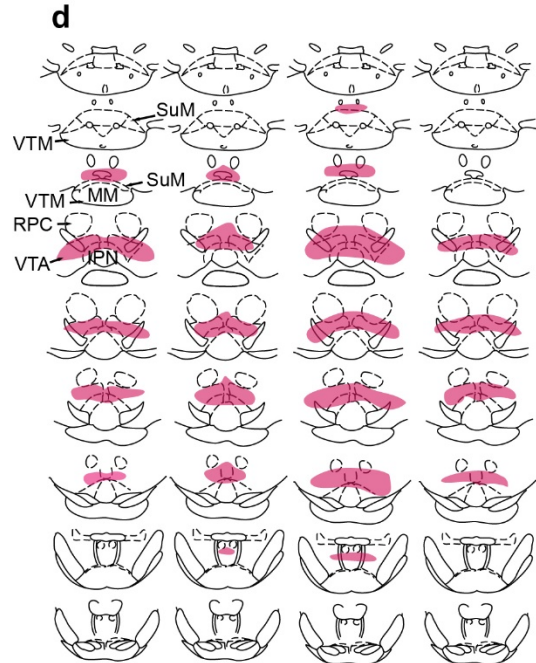
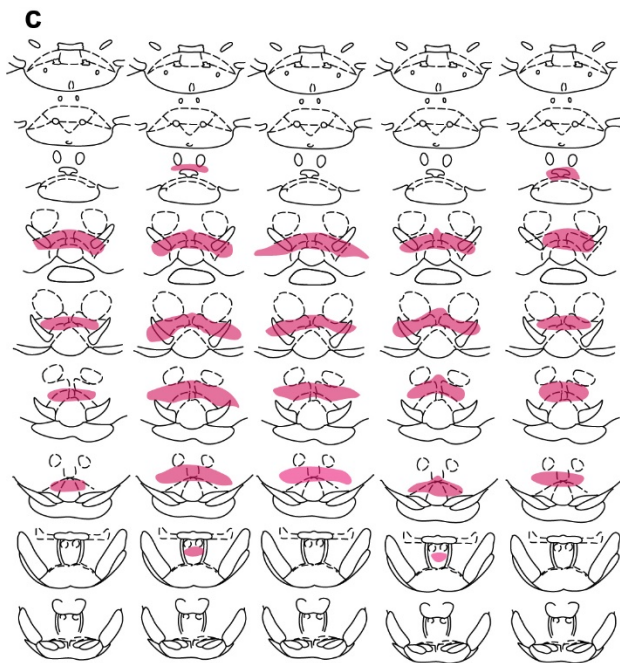
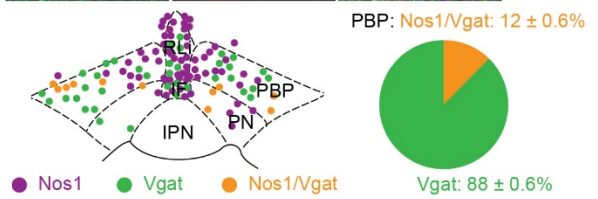
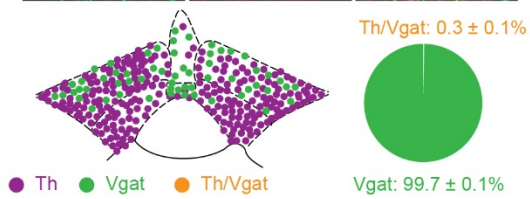
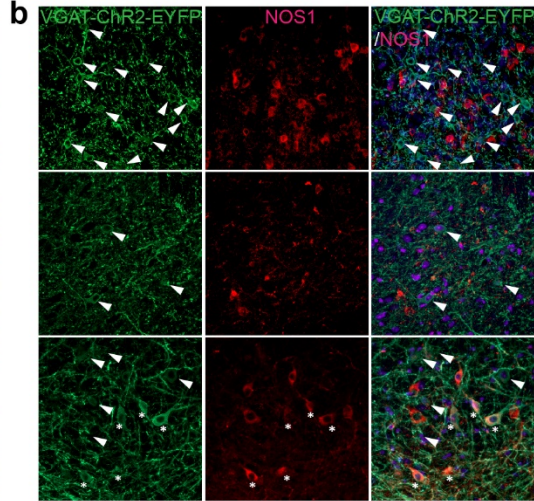
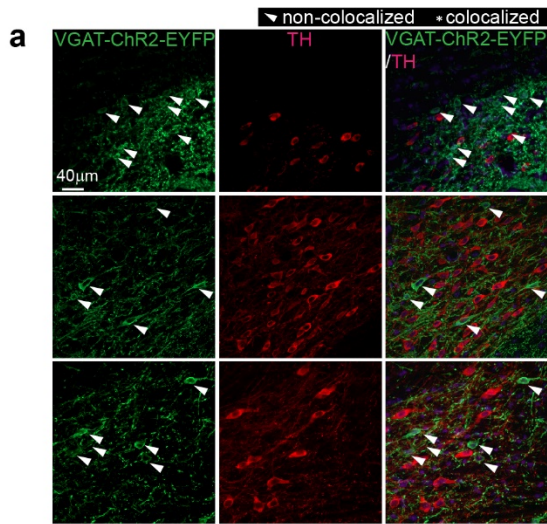
(d) Time of wake and NREM sleep from CNO or saline-injected VTA^{Nos1}-hM3Dq mice after dopamine receptor antagonist injections.

(e) Examples of EEG, EMG and delta power spectra from CNO or saline-injected VTA^{Nos1}-hM4Di mice. “Epoch” indicates the vigilance state: blue, wake; green, NREM sleep; magenta, REM sleep.

Optogenetic circuit mapping of VTA^{Nos1} neurons

(f) Injection of AAV-DIO-ChR2-EYFP into the VTA of the *Nos1-ires-Cre* mice. Circuit mapping for VTA^{Nos1}-ChR2-EYFP mice. The experiment was repeated independently 3 times. IF, interfascicular nucleus; PBP, parabrachial pigment nucleus. RLi, rostral linear nucleus; VP, ventral pallidum; NAc, nucleus accumbens; LH, lateral hypothalamus; LHb, lateral habenula;

**p<0.01, repeated measures two-way ANOVA and Bonferroni-Holm *post hoc* test. Error bars represent the SEM. For detailed statistics information, see Supplementary Table1.



Supplementary Fig. 9 (Associated with Fig. 5)

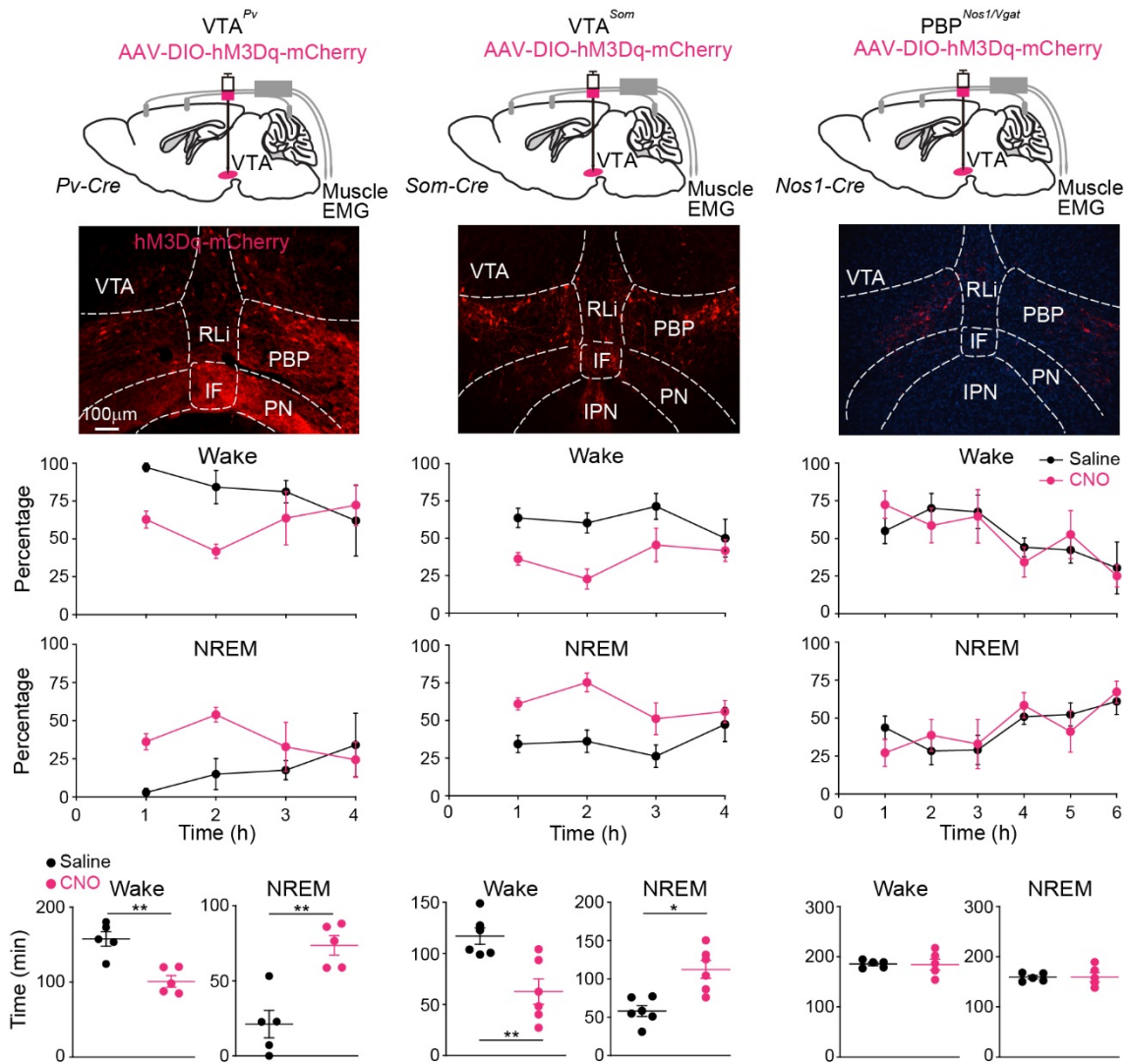
Immunocytochemical characterization of VTA^{Vgat} neurons

(a) In the VTA of VTA^{Vgat}-ChR2-EYFP mice, *Vgat*-expressing neurons are distinct from those expressing tyrosine hydroxylase (TH) (n=4 mice). Co-expression of EYFP and TH was rare. Data for pie chart represent mean \pm SEM.

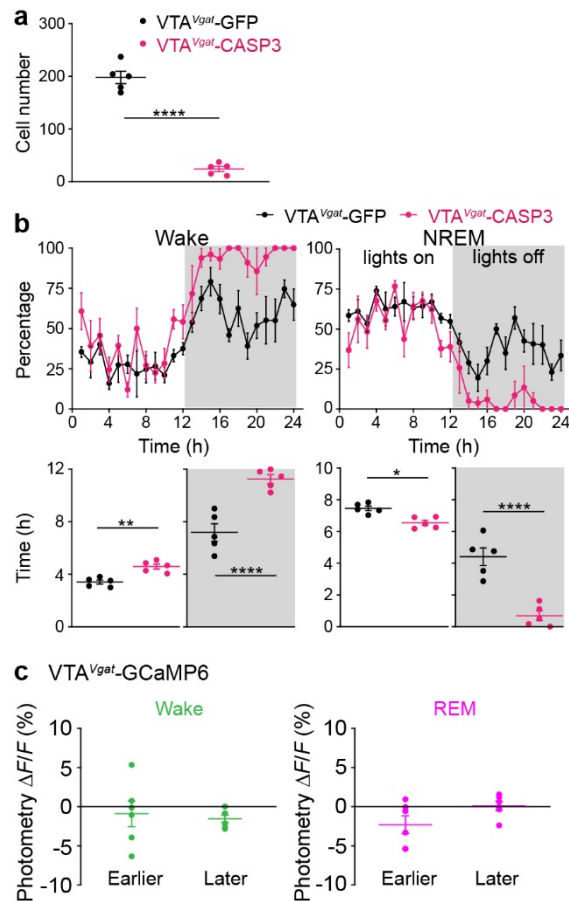
(b) In the midline VTA of VTA^{Vgat}-ChR2-EYFP mice, *Vgat*-expressing neurons are distinct from those expressing NOS1 (n=4 mice). Some VTA^{Vgat} cells in the PBP co-express NOS1 (12 \pm 0.6%). IF, interfascicular nucleus; RLi, rostral linear nucleus; PBP, parabrachial pigmented nucleus; PN, paranigral nucleus; IPN, interpeduncular nucleus. Data for pie chart represent as mean \pm SEM.

Examples of expression of hM3Dq-mCherry and hM4Di-mCherry expression in individual *Vgat-ires-Cre* mice

(c, d) Sections shown as line diagrams from individual mice, from anterior to posterior, with areas of hM3Dq-mCherry (c) or hM4Di-mCherry (d) receptor expression, shown schematically in magenta, in VTA^{Vgat}-hM3Dq or VTA^{Vgat}-hM4Di mice. IPN, interpeduncular nucleus; MM, medial mammillary area; RPC, red nucleus, parvocellular part. SuM, supramammillary area. VTM, ventral tuberomammillary nucleus.



* $p < 0.05$, ** $p < 0.01$; two-sided unpaired t-test. Error bars represent the SEM. For detailed statistics information, see Supplementary Table1.



Supplementary Fig. 11 (Associated with Fig. 6)

Sleep-wake patterns of VTA^{Vgat}-CASP3 mice

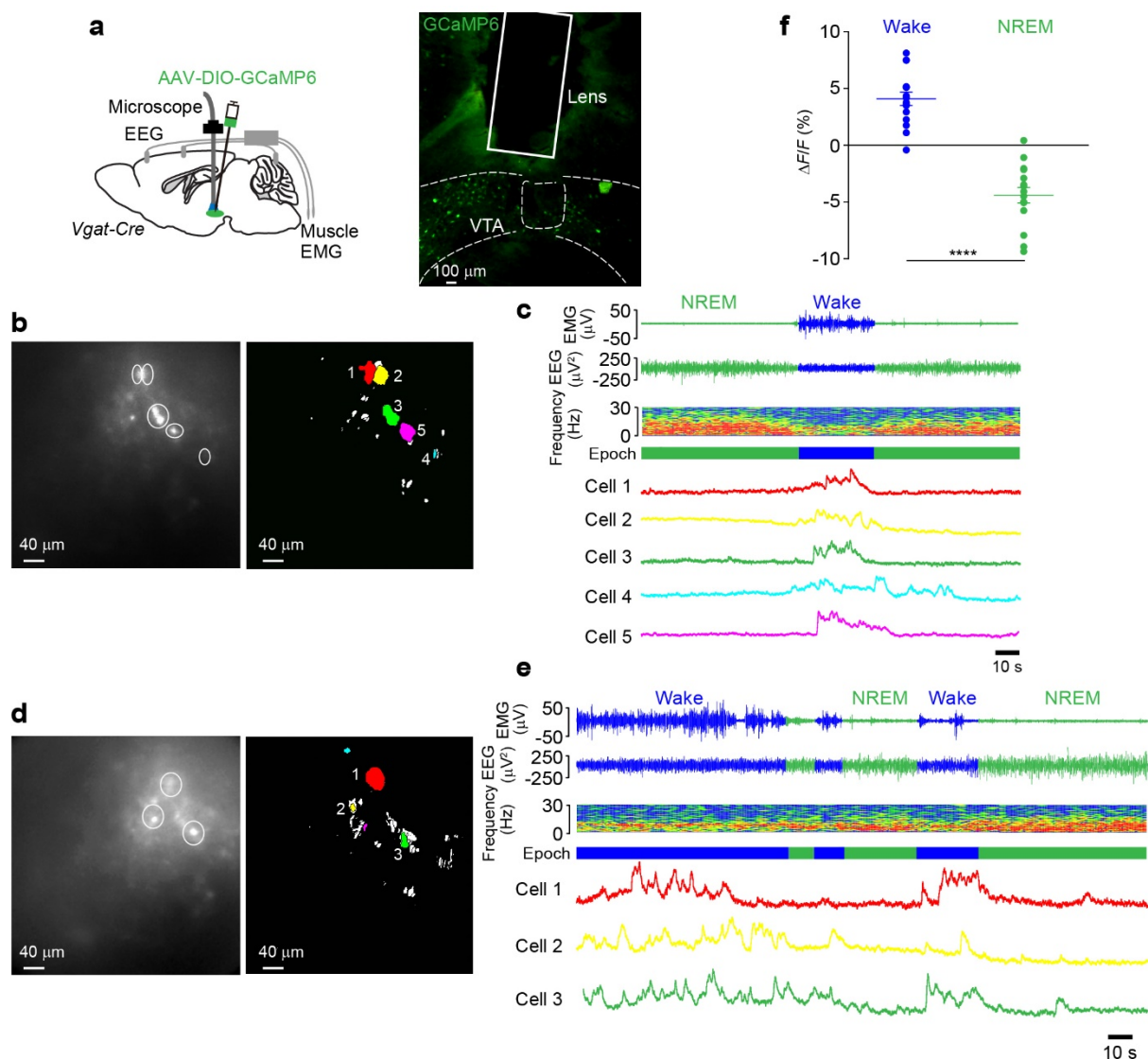
(a) GFP-positive cell numbers of VTA^{Vgat}-GFP mice (n=5 mice) and VTA^{Vgat}-CASP3 mice (n=5 mice).

(b) Percentage and time of wake, NREM or REM sleep of VTA^{Vgat}-GFP mice (n=5 mice) and VTA^{Vgat}-CASP3 mice (n=5 mice) 4 months after virus injection.

Ca²⁺ signals of VTA^{Vgat} neurons during individual bouts of REM sleep and wake

(c) Within an individual bout of wake or REM sleep, the Ca²⁺ signal of the VTA^{Vgat} cells during the earlier and later parts of the bout did not change significantly (n=6 mice; 95 sessions for wake and 131 sessions for REM sleep).

*p<0.05, **p<0.01, ****p<0.0001; two-sided for a and b, unpaired t-tests; for c, two-sided paired t-test. Error bars represent the SEM. For detailed statistics information, see Supplementary Table1.



Supplementary Fig. 12 (Associated with Fig. 6)

***In vivo* Ca^{2+} imaging of VTA^{Vgat} neurons and correlating their activity with vigilance state shows that VTA^{Vgat} neurons are wake-active**

(a) AAV-DIO-GCaMP6f was injected into the VTA area of *Vgat-ires-Cre* mice and a GRIN lens was implanted into the VTA. GCaMP6 expression can be detected in the VTA area. The trace of where the lens was placed is illustrated. The experiment was repeated independently 4 times.

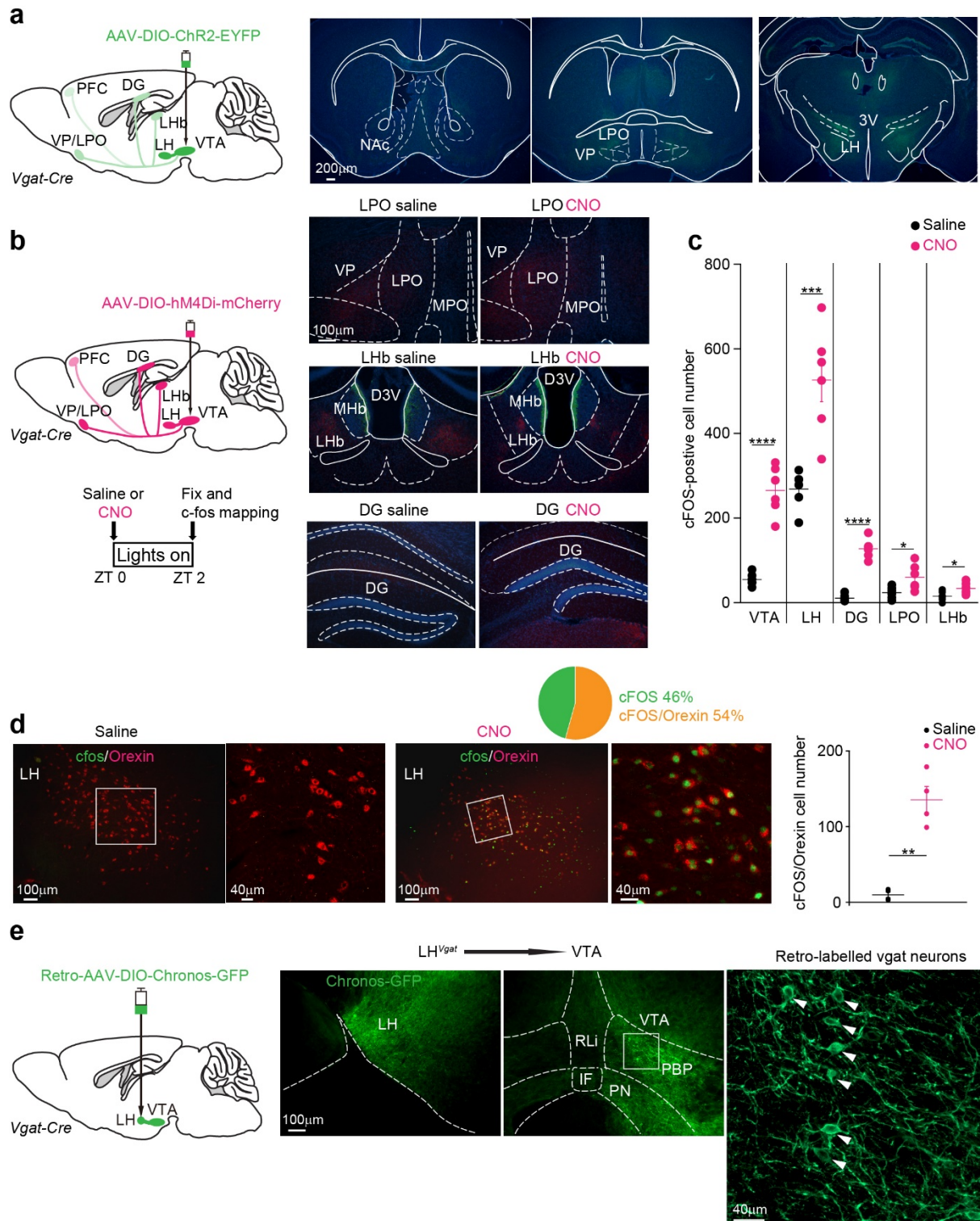
(b) An example of Ca^{2+} imaging and activity map indicating individual cells (colour-coded) that have been recorded.

(c) Ca^{2+} traces recorded in the imaging during NREM sleep or wakefulness for the cells shown in panel b. Examples of EEG, EMG and delta power spectra. “Epoch” indicates the vigilance state: blue, wake; green, NREM sleep.

(d) Another example of Ca^{2+} imaging and activity map indicating individual cells (colour-coded) that have been recorded.

(e) Ca^{2+} traces recorded in the imaging during NREM sleep or wakefulness for the cells shown in panel d. Examples of EEG, EMG and delta power spectra. “Epoch” indicates the vigilance state: blue, wake; green, NREM sleep.

(f) $\Delta F/F$ ratio of the Ca^{2+} photometry signal in $\text{VTA}^{\text{Vgat}}\text{-GCaMP6f}$ mice during wakefulness and NREM sleep (16 cells of 4 mice). **** $p < 0.0001$; two-sided paired t-test. Error bars represent the SEM. For detailed statistics information, see Supplementary Table1.



Supplementary Fig. 13 (Associated with Fig. 7, 8)

Chemogenetic and optogenetic circuit mapping of VTA^{Vgat} neurons

(a) Circuit mapping for VTA^{Vgat}-ChR2-EYFP mice in whole brain.

(b) Chemogenetic mapping with cFOS expression following inhibition of VTA^{Vgat} neurons. The number of cFOS neurons identified immunohistochemically (green dots) were counted (see graph in c) throughout the brain two hours after CNO or saline injection at ZT0 (start of “lights on”) in VTA^{Vgat}-hM4Di mice. The magenta/pink staining is the primary fluorescence of VTA^{Vgat} axons containing hM4Di-mCherry protein.

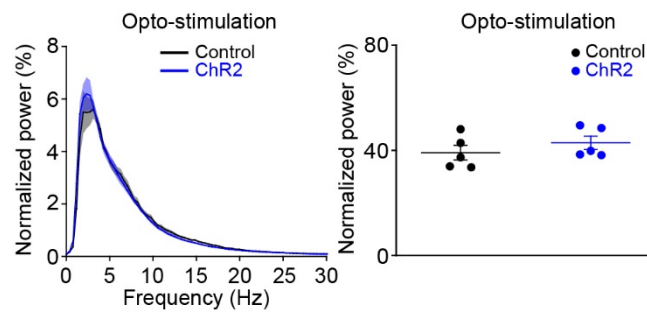
(c) cFOS induction in different brain areas of VTA^{Vgat}-hM4Di mice after saline (n=6 mice) or CNO (n=6 mice) *i.p.* injection.

(d) Double-labelling and quantification of cFOS and orexin immunocytochemistry in the LH area of VTA^{Vgat}-hM4Di mice 2 hours after saline (n=4 mice) or CNO *i.p.* injection (n=4 mice).

(e) Retro-AAV-DIO-Chronos-GFP was injected into the LH area of *Vgat-ires-Cre* mice. Images show GFP staining in the LH and VTA areas. White arrows indicate retro-labelled soma in the VTA.

VP, ventral pallidum; NAc, nucleus accumbens; LPO, lateral preoptic area; MPO, medial preoptic area; LH, lateral hypothalamus; LHb, lateral habenula; MHb, medial habenula; DG, dentate granule cells; D3V, dorsal 3rd ventricle; 3V, 3rd ventricle; IF, interfascicular nucleus; RLi, rostral linear nucleus; PBP, parabrachial pigmented nucleus; PN, paranigral nucleus; IPN, interpeduncular nucleus.

*p<0.05, **p<0.01, ***p<0.001, ****p<0.0001; two-sided unpaired t-test. Error bars represent the SEM. For detailed statistics information, see Supplementary Table1.

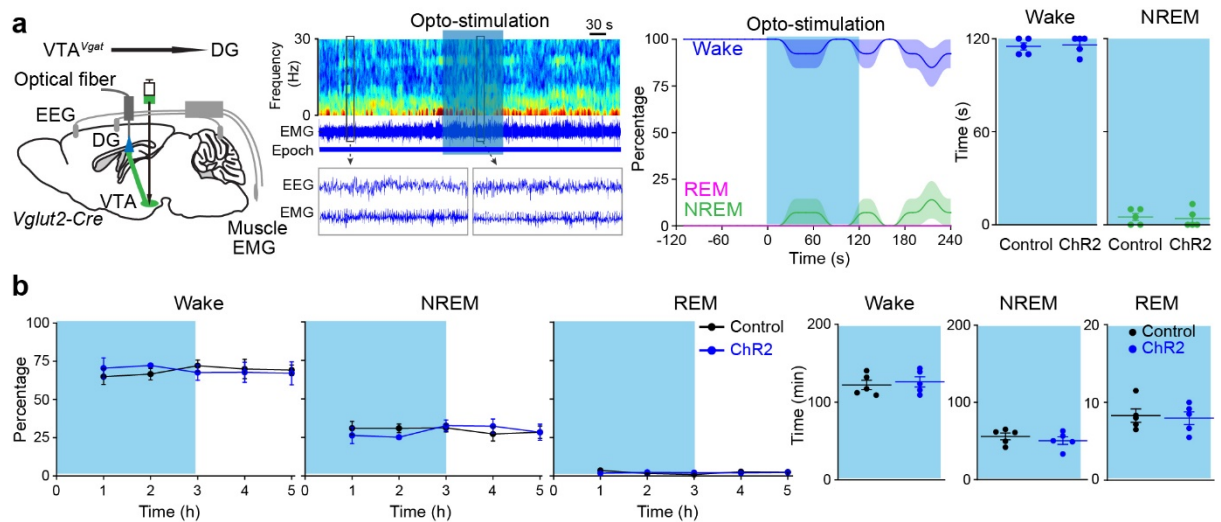


Supplementary Fig. 14 (Associated with Fig. 8)

EEG power spectrum during optogenetic activation of the VTA^{Vgat}→LH projection

EEG power spectrum and delta power (0.5-4 Hz) for NREM sleep during 5 min of opto-stimulation.

$p > 0.05$, two-sided unpaired t-test. Shaded regions represent SEM. All error bars represent the SEM. For detailed statistics information, see Supplementary Table1.

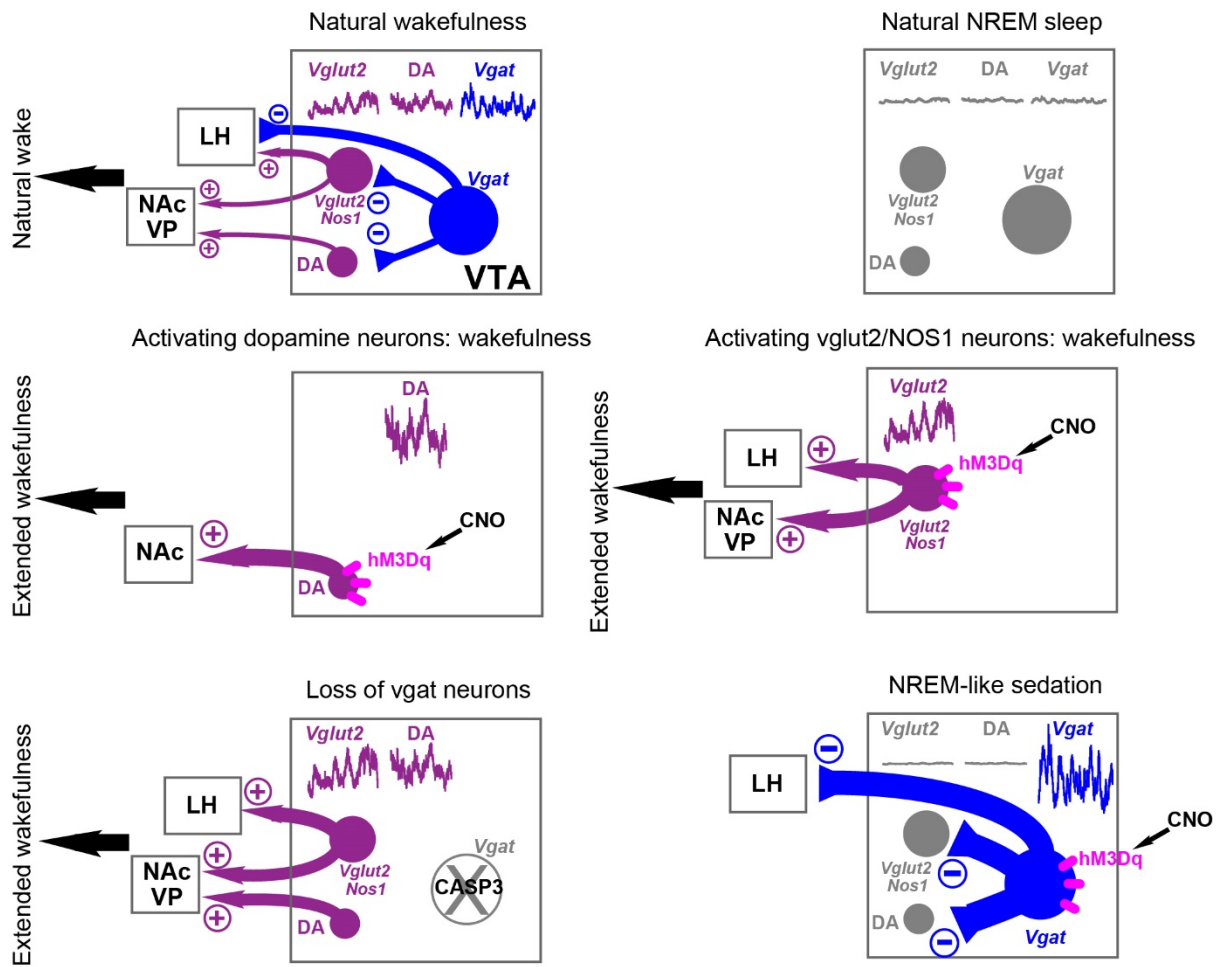


Supplementary Fig. 15 (Associated with Figs. 7 & 8)

Optogenetic activation of the VTA^{Vgat}→DG projection

(a, b) For activating the VTA^{Vgat}→DG projection, an optical fiber was placed into the DG area of VTA^{Vgat}-ChR2-EYFP mice. (a) Mice were given 120 s of opto-stimulation (20 Hz) during wakefulness and the percentage and time of wake and NREM were scored (control: n=5 mice; 10 trials; ChR2: n=6 mice; 13 trials). (b) mice (control: n=5 mice; ChR2: n=5 mice) were given 3 hours of opto-stimulation during wake period and the percentage and time of wake, NREM and REM sleep were scored.

$p > 0.05$, for a and b, two-sided unpaired t-test. Shaded regions represent SEM. All error bars represent the SEM. For detailed statistics information, see Supplementary Table1.



Supplementary Fig. 16 (Associated with Figs. 1-8)

Conceptual circuit diagrams illustrating a hypothesis of how VTA^{Vgat}, VTA^{Vglut2} and VTA^{DA} neurons contribute to the regulation of vigilance states

The top left-hand box shows the situation in wakefulness. In the VTA, VTA^{Vglut2/Nos1}, VTA^{Vgat} and VTA^{DA} neurons are all selectively wake (and REM-sleep) active⁵. The top right-hand box illustrates that during natural NREM sleep, all types of neurons in the VTA are silent or less active (as indicated by grey shading). The traces are schematics of the Ca²⁺ photometry signals for the different sorts of neurons in the VTA. The photometry signal for DA neurons is inferred from ref⁵. During wakefulness, the hypothesis is that the VTA^{Vglut2/Nos1} and VTA^{DA} neurons are contributing to the generation of wakefulness by exciting the nucleus accumbens shell (NAc)/ventral

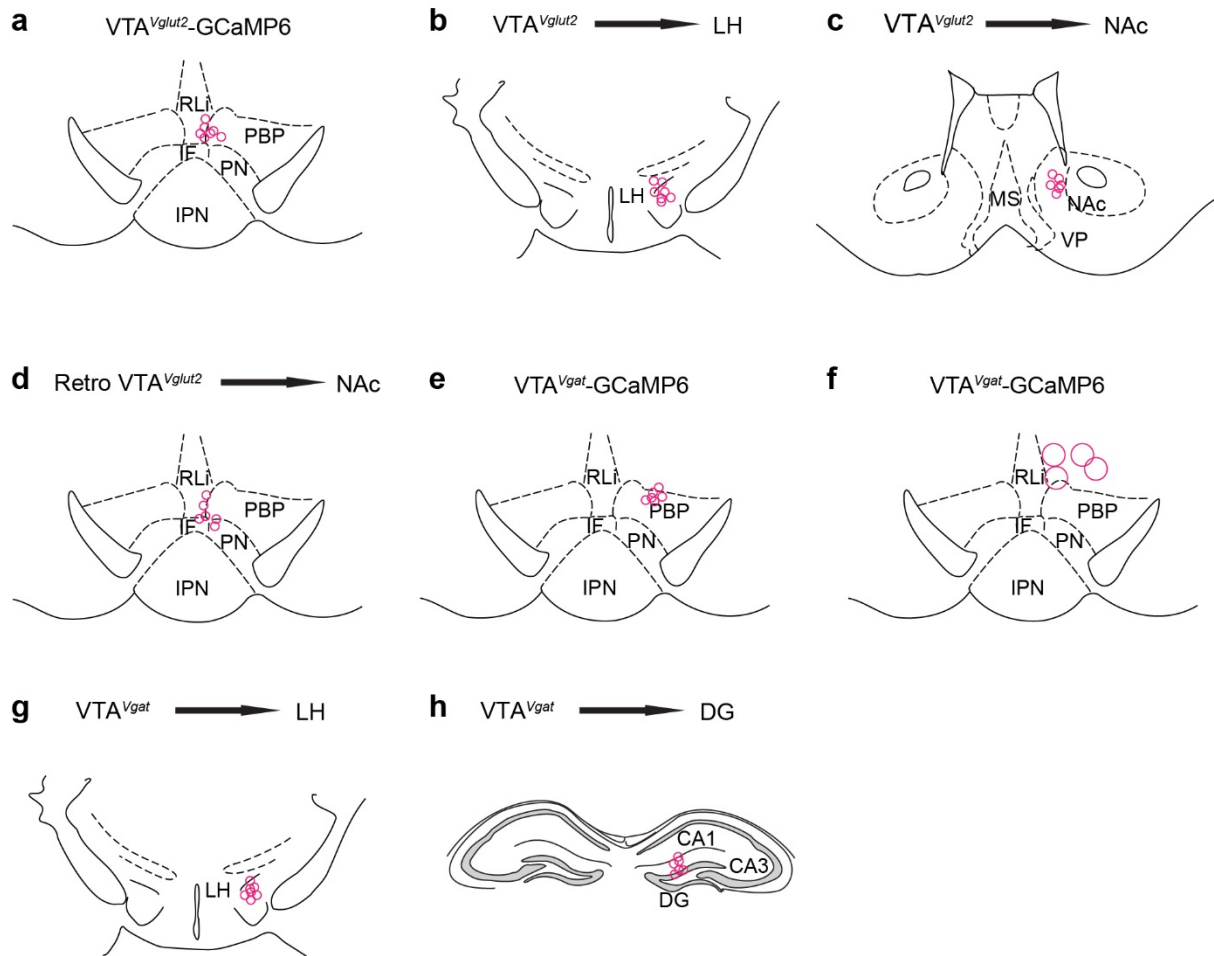
pallidum (VP) and orexin neurons in the lateral hypothalamus (LH). VTA^{Vgat} neurons would be providing an ongoing inhibitory tone onto the $VTA^{Vglut2/Nos1}$ and VTA^{DA} neurons, as well as to the lateral hypothalamus. The consequence of this wake-on inhibitory tone is that the extent of wakefulness is limited.

The middle left-hand box summarizes data that selective chemogenetic activation of VTA^{DA} neurons produces wake⁸, as does their selective optogenetic activation⁵.

The middle right-hand box shows that chemogenetically activating $VTA^{Vglut2/Nos1}$ neurons alone also induces wakefulness (our study).

The bottom left-hand box illustrates that pathological loss of the VTA^{Vgat} neurons (using caspase) produces extended wakefulness. The loss of sleep lasts for many months. A hypothesis is that this is because of loss of inhibition onto the $VTA^{Vglut2/Nos1}$, VTA^{DA} neurons and the LH.

The bottom right-hand box shows the converse from lesioning the VTA^{Vgat} neurons. The selective activation of VTA^{Vgat} neurons, in this case chemogenetically with CNO, produces a profound NREM-like sedation. Our results suggest that this is because of inhibition of the LH and $VTA^{Vglut2/Nos1}$ and VTA^{DA} neurons.



Supplementary Fig. 17 (Associated with Figs. 1-8)

Fiber placements for the optogenetic and photometry experiments

- (a) Fiber placement in the VTA for the $VTA^{Vglut2}\text{-GCaMP6}$ mice.
- (b) Fiber placement in the LH for the activation of the $VTA^{Vglut2}\rightarrow LH$ projections.
- (c) Fiber placement in the NAc for the activation of the $VTA^{Vglut2}\rightarrow NAc$ projections.
- (d) Fiber placement in the VTA for the activation of the retro $NAc^{Vglut2}\rightarrow VTA$ projections.
- (e) Fiber placement in the VTA for the $VTA^{Vgat}\text{-GCaMP6}$ mice.
- (f) GRIN lens placement in the VTA for the $VTA^{Vgat}\text{-GCaMP6}$ mice.
- (g) Fiber placement in the LH for the activation of the $VTA^{Vgat}\rightarrow LH$ projections.
- (h) Fiber placement in the DG for the activation of the $VTA^{Vgat}\rightarrow DG$ projections.

DG, dentate granule cells; IF, interfascicular nucleus; IPN, interpeduncular nucleus; LH, lateral hypothalamus; NAc, nucleus accumbens; PBP, parabrachial pigmented nucleus; PN, paranigral nucleus; RLi, rostral linear nucleus; VP, ventral pallidum.